Original Article

MOLECULAR METABOLISM

miR-126 contributes to the epigenetic signature of diabetic vascular smooth muscle and enhances antirestenosis effects of Kv1.3 blockers

Marycarmen Arevalo-Martinez [1,2,7], Pilar Cidad [1,2], Sara Moreno-Estar [1,2], Mirella Fernández [3], Sebastian Albinsson [4], Irene Cózar-Castellano [1,2,5], José R. López-López [1,2,6], M. Teresa Pérez-Garcia [1,2,*,6]

ABSTRACT

Objectives: Restenosis after vessel angioplasty due to dedifferentiation of the vascular smooth muscle cells (VSMCs) limits the success of surgical treatment of vascular occlusions. Type 2 diabetes (T2DM) has a major impact on restenosis, with patients exhibiting more aggressive forms of vascular disease and poorer outcomes after surgery. Kv1.3 channels are critical players in VSMC proliferation. Kv1.3 blockers inhibit VSMCs MEK/ERK signalling and prevent vessel restenosis. We hypothesize that dysregulation of microRNAs (miR) play critical roles in adverse remodelling, contributing to Kv1.3 blockers efficacy in T2DM VSMCs.

Methods and results: We used clinically relevant in vivo models of vascular risk factors (VRF) and vessels and VSMCs from T2DM patients.

Resukts: Human T2DM vessels showed increased remodelling, and changes persisted in culture, with augmented VSMCs migration and proliferation. Moreover, there were downregulation of PI3K/AKT/mTOR and upregulation of MEK/ERK pathways, with increased miR-126 expression. The inhibitory effects of Kv1.3 blockers on remodelling were significantly enhanced in T2DM VSMCs and in VRF model. Finally, miR-126 overexpression confered "diabetic" phenotype to non-T2DM VSMCs by downregulating PI3K/AKT axis.

Conclusions: miR-126 plays crucial roles in T2DM VSMC metabolic memory through activation of MEK/ERK pathway, enhancing the efficacy of Kv1.3 blockers in the prevention of restenosis in T2DM patients.

Keywords Vascular remodeling; Type 2 diabetes mellitus; Vascular smooth muscle; Kv1.3 channel blockers; miRNAs; Cell proliferation

1. INTRODUCTION

Coronary artery bypass graft (CABG) surgery is used to relieve consequences associated with ruptured or occlusive coronary artery atherosclerotic plaques. The surgery uses undiseased vessels for the diversion of blood from the aorta to the coronary artery. However, the long-term efficacy of bypass grafts remains restricted owing to complete or significant occlusion (restenosis) of the conduits. Mechanical injury triggers repair mechanisms, which leads to excessive vascular smooth muscle cell (VSMC) migration and proliferation in the intima of the vessel graft. Atherothrombotic cardiovascular disease is the leading cause of death worldwide and the ongoing epidemic of obesity-induced insulin resistance and type 2 diabetes mellitus (T2DM) contributes to its increased rate. T2DM is associated with an increased prevalence of coronary artery disease and it is an independent risk factor for poor outcomes following CABG, with higher morbidity and short- and long-term mortality [1]. Although preventive medicine seeks to reverse this trend, complementary approaches that identify potential therapeutic targets relevant to vascular disease in T2DM are required.

The enhanced vascular response in T2DM is partly because of a proinflammatory and pro-proliferative environment, potentiated by hyperinsulinemia and other metabolic disarrangements. While early glycemic control can retard microvascular disease in T2DM [2], macrovascular complications persist, particularly in patients with active coronary heart disease [3]. Uncontrolled hyperglycemia can leave an early imprint on vascular cells, the metabolic memory [4], whose deleterious effects persist for a long time after effective glycemic control [5]. The mechanisms involved in the T2DM epigenetic signature in the vasculature remain ill-defined.

[1]Departamento de Bioquímica y Biología Molecular y Fisiología, Universidad de Valladolid, Valladolid, Spain [2]Unidad de Excelencia, Instituto de Biología y Genética Molecular (IBGM), CSIC, Valladolid, Spain [3]Cardiovascular Surgery Department, Hospital Clínico Universitario de Valladolid, Spain [4]Department of Experimental Medical Science, University of Lund, Sweden [5]CIBERDEM Centro de Investigación Biomédica en Red de Diabetes y Enfermedades Metabólicas Asociadas, Madrid, Spain

[6] Equal senior authors.
[7] Present address: Department of Experimental Medical Science, University of Lund, Sweden.

*Corresponding author. Departamento de Bioquímica y Biología Molecular y Fisiología, Universidad de Valladolid, Edificio IBGM, c/ Sanz y Forés, 3, 47003 Valladolid, Spain. E-mail: tperez@ibgm.uva.es (M.T. Pérez-Garcia).

Received May 24, 2021 • Revision received July 9, 2021 • Accepted July 15, 2021 • Available online 20 July 2021

https://doi.org/10.1016/j.molmet.2021.101306

Abbreviation

VSMCs	Vascular Smooth Muscle Cells
T2DM	Type 2 Diabetes Mellitus
CABG	Coronary Artery Bypass Graft
PM	Phenotypic Modulation
IH	Intimal Hyperplasia
hMA	Human Mammary Artery
hRA	Human Renal Artery
PAP-1	5-(4-phenoxybutoxy) psoralen
BPH	Blood Pressure High
BPN	Blood Pressure Normal
HFD	High-Fat Diet
iPGTT	Intraperitoneal Glucose Tolerance Test
iPITT	Intraperitoneal Insulin Tolerance Test
EVL	Everolimus

VSMCs express contractile proteins which allow vascular tone control by the regulation of vessel diameter [6]. In response to local cues, VSMCs can switch to a dedifferentiated phenotype, acquiring migratory and proliferative capabilities. While this phenotypic modulation (PM) is fully reversible in healthy vessels [7], the inherent plasticity of VSMCs also contributes to vascular diseases and intimal hyperplasia (IH) development.

Kv1.3 channels represent novel targets for the treatment of unwanted remodeling [8–10]. Selective Kv1.3 blockade inhibits PM and prevents restenosis in animal models of vascular lesions [11] and in human vessels [12]. However, its efficacy in vessels with underlying diseases awaits confirmation. VSMCs PM is also regulated by miRNAs, which can contribute to the development of vasculoproliferative diseases and also to the detrimental vascular phenotype associated with diabetes [13–16]. It has been suggested that exacerbation of VSMCs dedifferentiation in T2DM is mediated by a specific miRNA signature. The concerted action of these dysregulated miRNAs contributes to the multifactorial vascular response in diabetes.

Here, we used human mammary artery (hMA) samples to compare vessel remodeling and VSMCs migro-proliferative responses between non-T2DM and T2DM patients. The observed differences led us to explore the miRNA signature of T2DM VSMCs. We found that miR-126-3p was differentially regulated in T2DM vessels upon PM. miR-126 expression decreased in contractile T2DM VSMCs from the wall of the vessels, but was among the most upregulated miRNAs in T2DM VSMCs cultures. miR-126 overexpression in non-T2DM recapitulates VSMCs T2DM phenotype in cell migration and proliferation. Moreover, the inhibition of PM with the Kv1.3 blocker, PAP-1, was significantly larger in T2DM samples and non-T2DM VSMCs, overexpressing miR-126. Kv1.3 blockers also exhibit increased potency and prevent restenosis of T2DM vessels *in vivo*. Altogether, our data indicate that miR-126 upregulation is an essential element contributing to metabolic memory of T2DM VSMCs, acting through Kv1.3-dependent mechanisms.

2. METHODS

2.1. Human samples

The hMA samples from the COLMAH collection (https://www.redheracles.net/plataformas/en_coleccion-muestras-arteriales-humanas.html) were obtained from donors undergoing CABG at the Clinic Hospital of Valladolid, together with associated anonymized data. Protocols in accordance with the Helsinki Declaration, which included prior informed written consent, were approved by the Hospital Ethics Committee. Samples from 28 patients (13 T2DM and 15 non-T2DM) were included in this study (refer Table 1 for clinical information).

For organ culture, 5 mm wide rings of hMA were incubated for 2 weeks as described [12], using sequential sections of the same artery for the different experimental conditions. Afterward, rings were fixed with 4 % formaldehyde for morphometric analysis or saved in RNAlater™ (Thermo Fisher) for expression studies.

VSMC primary cultures were obtained from explants of hMA or human renal arteries (hRA, from COLMAH collection) as described [17]. VSMCs in passages 3–10 were used for experiments. For high glucose treatment, VSMCs were incubated for 24–48 h in 22 mM glucose containing-media.

2.2. Animal models

BPH (blood pressure high) and BPN mice (blood pressure normal) – both from Jackson Laboratories – were maintained by inbreeding crossing. All procedures were approved by the Animal Care and Use Committee of the University of Valladolid (Project 505649), in accordance with the European Community guides (Directive 2010/63/UE).

To generate a VRF model, 6 weeks old BPH mice were fed with a standard rodent chow diet (SD) or high-fat diet (HFD; Research Diets, #D12492, 60 % fat) for 12 weeks. Weight, blood pressure, fasting blood glucose, intraperitoneal glucose tolerance test (ipGTT), and intraperitoneal insulin tolerance test (ipITT) [18] were determined (see expanded methods). To induce IH, carotid artery ligation was performed as described [19]. Four weeks after surgery, animals were euthanized in a CO_2 chamber. Some experimental groups were treated with the Kv1.3 blocker PAP-1 (5-(4-phenoxybutoxy) psoralen) or the mTOR blocker everolimus (EVL).

2.3. Morphometric studies

Fixed arteries were paraffin-embedded to obtain 7-μm sections [12,19]. Vascular remodeling and IH development were determined in Masson trichrome stained sections using well-known descriptors [19,20] (refer Supplemental Figure I and Table 1).

2.4. RNA expression

Total RNA was extracted from VSMCs culture and vessel segments with TRIzol® (Ambion). mRNA expression of Kv1.3 and several miR-126 putative target genes (refer Supplemental table III) was determined with qPCR with Taqman assays (Applied Biosystems) using RPL18 (ribosomal L18) as housekeeping [12].

miRNeasy Mini Kit (Qiagen) and miScript II RT kit (Qiagen) were used for microRNA isolation and reverse transcription, respectively. miScript SYBR® Green PCR kit(Qiagen) was used for the detection of pre-miR-126 and mature miRNAs, using snord-68 as housekeeping. For plasma miR-126 determinations, Ce-miR-39 was added as the spike-in control. The relative abundance quantification method ($2^{-\Delta\Delta CT}$) was used in all cases [21].

The miScript miRNA PCR Array focused on human cardiovascular disease (Qiagen, MIHS-113Z) was used to identify T2DM dysregulated miRNAs, using the StepOnePlus™ Real-Time PCR System. Data analysis was conducted at QIAGEN's Gene Globe Data Analysis Center using the miScript miRNA PCR Array data analysis tool.

2.5. Protein expression

For western-blot experiments, VSMCs preincubated 24 h with serum-free media were stimulated with 100 nM insulin for 15 or 30 min. Immunohistochemistry experiments were carried out as described [12] (refer also Supplemental methods).

Table 1 — Summary of clinical data from the hMA donors for organ culture, primary VSMC cultures, or both.

Parameter (MEAN ± SEM)	Total (n = 28)	T2DM (n = 13)	NoN-T2DM (n = 15)	p-value
Age (yrs)	68.55 ± 1.53	68.69 ± 2.13	68.44 ± 2.24	0.936
Min	51	51	52	
Max	83	78	83	
Gender (%)				
Male	82.14	76.92	86.67	0.305
Female	17.86	23.08	13.33	
BMI (KG/M^2)	27.75 ± 0.75	27.61 ± 1.17	27.87 ± 1.00	0.923
Blood Pressure (mmHg)				
Systolic	128.72 ± 4.63	130.50 ± 6.65	127.30 ± 6.70	0.742
Diastolic	76.33 ± 3.65	72.88 ± 4.45	79.10 ± 5.57	0.413
Mean	93.80 ± 3.76	92.08 ± 4.89	95.17 ± 5.72	0.696
Glycemia (mg/dL)	123.85 ± 8.63	146.38 ± 15.25	102.93 ± 4.27	**0.0089**
T2DM treatment (%)				
Diet		15.38		
Oral Antidiabetics		53.85		
Insulin		30.77		
Cardiovascular risk factors (%)				
Hypertension	73.90	91.60	54.55	**0.0428**
Dyslipemia	73.68	88.90	60.00	0.162
Smoking	15.79	11.11	20.00	0.418
Previous MI	47.37	66.66	30.00	0.056
Previous Angina	68.42	55.55	80.00	0.209
Previous stroke	5.56	11.11	0.00	0.5
PVD	22.22	44.44	0.00	**0.041**

Significant values are in bold (p-values from Fisher exact test). BMI = Body mass index; MI = myocardial infarct; PVD = peripheral vascular disease.

2.6. Proliferation and migration assays

Proliferation was induced by the addition of PDGF (20 ng/ml) alone or with PAP-1 (100 nM) for 24 h and quantified using EdU (5-ethynyl-2′-deoxyuridine) incorporation for 6 h with Click-iT® EdU Proliferation Assay (Invitrogen) as described [12]. Scratch migration assay was carried out in confluent VSMCs [12]; refer also supplemental methods.

2.7. miRNA gain of function experiments

The mirVanaTM miRNA mimics were used to overexpress hsa-miR-126-3p (MH12841, Ambion) in VSMCs. VSMCs at 80—90 % confluence were transfected with 10 nM of miR-126 mimic or mimic negative control (C-) with Lipofectamine 2000 (Thermo Fisher), and used for expression and functional studies after 24 h.

2.8. Statistics

Data were plotted and analyzed using Origin (OriginLab Corp), Excel, and R software as previously described [12] (refer supplemental methods). Pooled data are represented with box plots indicating the mean (as an X), the median value, the SE (the size of the box), and the SD (the whiskers). Individual determinations are also shown and p-values$<$0.05 were considered significantly different. For comparisons between two groups with normal distribution and equal variance, Student's t-test, for paired or unpaired data as required, was used to determine p-values. Welch's t-test was applied in the case of normal distribution and unequal sample size and variance, and Wilcoxon—Mann—Whitney test was used for nonparametric distributions. For comparisons among several groups, one-way ANOVA followed by Tukey's test was employed in the case of normal distributions and equal variances; alternatively, Kruskal—Wallis analysis followed by Dunn's test was also used. Shapiro—Wilk test and Bartlett's test were used to test the normality and homogeneity of variances, respectively. Fisher's exact test was used for the analysis of categorical data.

2.9. Ethics approval and consent to participate

The Animal Ethics Care and Use Committee of the University of Valladolid (Project 505649), which conforms to the guidelines from Directive 2010/63/EU of the European Parliament on the protection of animals used for scientific purposes approved all animal procedures used in this study. The human arteries of patients with or without T2DM with coronary artery disease (CAD) were obtained from donors undergoing CABG at the Clinic Hospital of Valladolid. Together with associated anonymized data, written informed consent were collected. Protocols were approved by the Hospital Ethics Committee in accordance with the Helsinki Declaration.

3. RESULTS

3.1. Effects of T2DM on human VSMC remodeling

The *ex vivo* organ culture model was used to explore remodeling [12]. The hMA rings from non-T2DM and T2DM patients were incubated for two weeks in organ culture. Approximately 20 % FBS induced marked remodeling, with increased wall thickness and neointima development. IH was more pronounced in the T2DM samples, which showed more than a two-fold increase of the intima to media ratio (I/M ratio) compared to control vessels (Figure 1A). VSMCs from T2DM vessels also showed increased expression of Kv1.3 mRNA (Figure 1B). We determined whether the differences in organ culture remain in primary VSMCs cultures obtained from those vessels and kept in identical conditions. T2DM VSMCs showed increased migration rates when compared to non-T2DM cultures (Figure 1C). Also, PDGF-induced proliferation was significantly increased in T2DM VSMCs from hMA or hRA compared to non-T2DM VSMCs (Figure 1D). These results — observed in 6—20 independent assays from at least 4 different patients in each group — suggest that T2DM induces permanent epigenetic changes in VSMCs cultures.

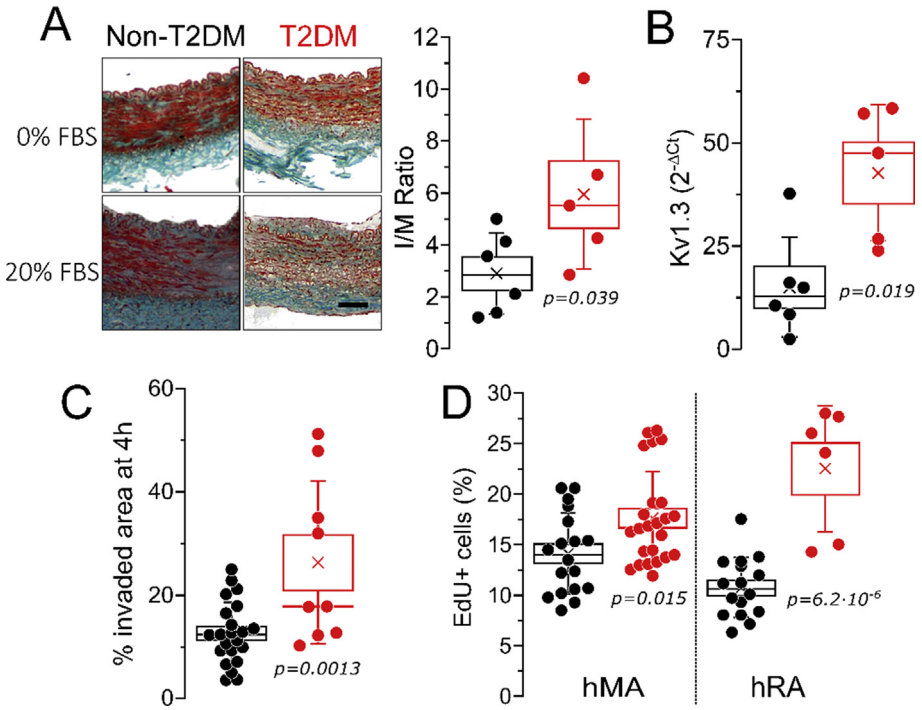

Figure 1: Phenotypic modulation is increased in T2DM VSMCs. A. Intima/media ratio of the hMA vessels kept in organ culture. All through the figures, the boxes mark the SEM range, the whiskers the SD, and the mean value is indicated by the X; n = 11 vessels, (6 non-T2DM and 5 T2DM); $p < 0.05$ Welch's t-test. Representative microphotographs of Masson trichrome-stained hMA sections after 2 weeks in 0 % or 20 % FBS are also shown. 10× objective, scale bar = 100 μm. **B.** Plot of Kv1.3 mRNA relative abundance to RPL18 in VSMCs from the media layer of hMA; n = 5–6 triplicate determinations, p-value from Welch's t-test. **C.** Migration rate obtained from scratch assays in 9–20 independent experiments from at least 4 different cell lines in each group, expressed as % of the invaded area; Welch's t-test. **D.** PDGF-induced proliferation in VSMCs cultures from hMA and hRA expressed as % of EdU-stained cells; n = 6–24 independent experiments in triplicate determinations; p values compared to non-T2DM samples are obtained from t-test.

3.2. Molecular mechanisms involved in T2DM epigenetic changes in VSMC

The phosphoinositide 3-kinase (PI3K/AKT/mTOR) and the extracellular signal-regulated kinase (MAPK/ERK) pathways mediated VSMC PM [9]. Reductions of insulin-stimulated insulin receptor substrate (IRS)-1 phosphorylation and IRS-1-associated PI3K activity in VSMCs have been described in T2DM [22]. Moreover, PI3K-dependent signaling regulated insulin metabolic functions, whereas Ras/MAPK pathways are involved in mitogenic effects of insulin and other growth factors. A reduction of the PI3K/AKT pathway would overdrive the unaffected MAPK–dependent pathways, leading to an imbalance between their functions [23,24], which could explain enhanced PM in diabetic patients. As Kv1.3 proliferative signaling in VSMCs is mediated through ERK activation [9], these changes could also influence the effects of Kv1.3 blockers in T2DM VSMCs. To explore this aspect, we checked the expression of some elements of these pathways. While AKT or IR phosphorylation in response to insulin was significantly reduced in T2DM, ERK1/2 phosphorylation was increased (Figure 2A). To identify the mechanisms involved, we screened the expression of 84 miRNAs with a qPCR array (Supplemental Table II) in non-T2DM and T2DM hMA VSMCs cultures (Figure 2B). Differentially expressed miRNAs were identified using the criteria of minimum reads <27 Ct and fold change ≥ 1.5. Three out of the five top differentially regulated miRNAs (miR-126, miR-1, miR-182) were validated by RT-qPCR using different T2DM and non-T2DM cultures (Supplemental Figure II).

Among the most dysregulated miRNAs in T2DM VSMCs, miR-126 was the most abundantly expressed. miR-126 has been described as a potential biomarker of diabetes risk and/or vascular complications of T2DM [15,25–28], but always associated with endothelial dysfunction [29]. To confirm miR-126 origin, we determined the expression levels of its precursor (pre-miR-126). Pre-miR-126 is expressed in VSMCs and upregulated in T2DM cultures (Figure 2C). Labeling with VSMC-specific markers such as SM alpha actin (SMA) and SM 22 alpha protein (Transgelin, SM22) confirmed the purity of our VSMC cultures (Figure 2D). Notably, non-T2DM VSMC incubated with high glucose (a widely used model of *in vitro* hyperglycemia [14,30,31]) did not exhibit miR-126 upregulation (Figure 2E).

These results suggested that miR-126 could be involved in epigenetic changes in T2DM VSMCs. We explored this possibility by analyzing the miR-126 overexpression effect on cell proliferation and migration. Mimic miR-126 upregulates miR-126 expression to a similar extent in both T2DM and non-T2DM VSMCs (Supplemental Figure III), but induced a significant increase in migration and proliferation only in non-T2DM VSMCs (Figure 3A,B). However, the proliferation rate of non-T2DM VSMCs overexpressing miR-126 was not different from the proliferation rate of T2DM cells. miR-126 overexpression led to AKT2 and PI3KR2, downregulation in non-T2DM cultures (Figure 3C). Moreover, western blot of extract from these cells also showed a significant decrease of AKT and its insulin-induced phosphorylated form in the cells transfected with mimic miR-126 (Figure 3D). Consistent with the observation that miR-126 targets in the insulin

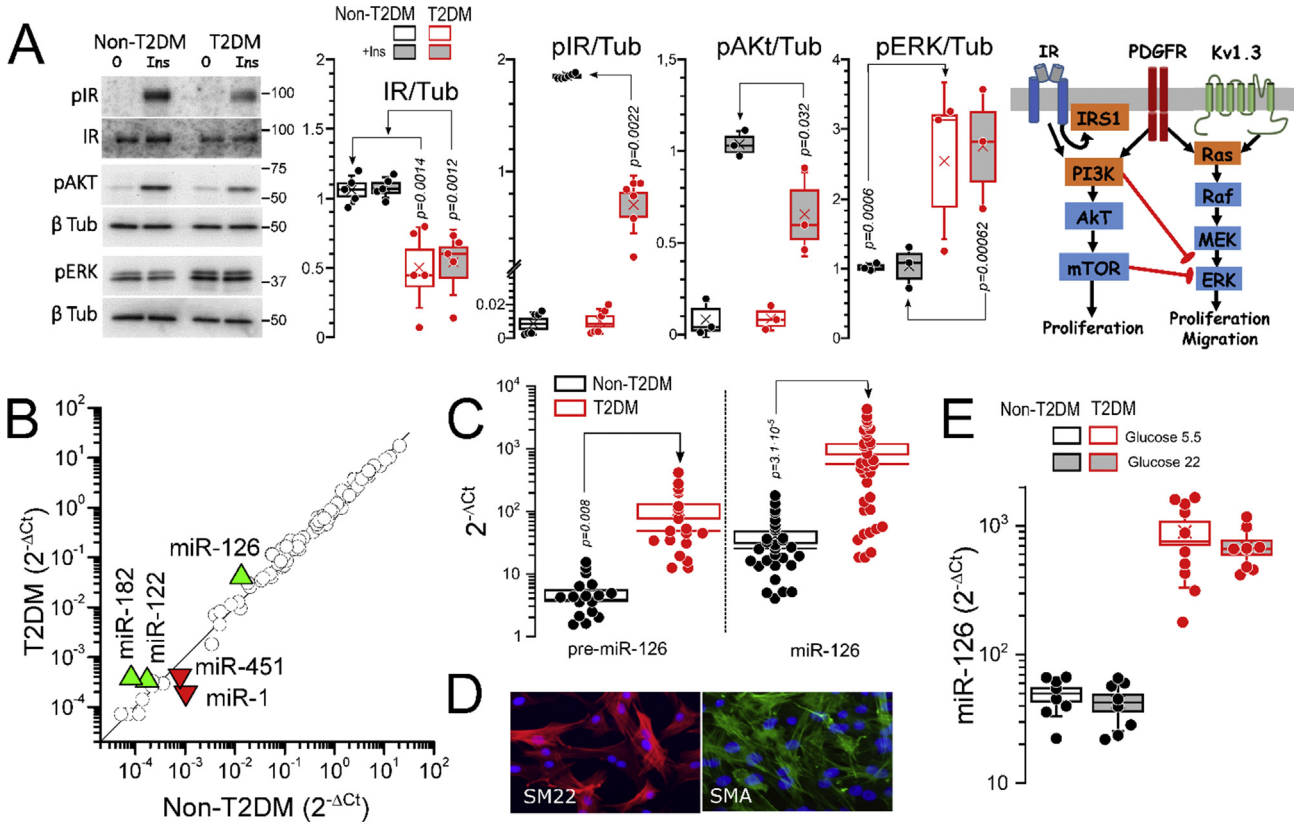

Figure 2: Altered signaling pathways and miR-126 dysregulation associates with metabolic memory in T2DM VSMC cultures. A. Representative Immunoblots of phosphorylated insulin receptor (pIR), phosphorylated AKT (pAKT), and phosphorylated ERK (pERK) from cultured VSMC incubated for 10 min with or without insulin (100 nM) as indicated. The boxplots show normalized data (n = 3–5); p values were obtained from multiple comparison tests using Kruskal–Wallis analysis followed by Dunn's test (for pIR) or one-way ANOVA and Tukey's test (for all other groups). A scheme of the signaling pathways explored is included. **B.** Plot of miRNA expression levels in T2DM versus non-T2DM cultured VSMC. Data were obtained from 2 different cultures in each group. Selected miRNAs with expression changes >1.5 fold are indicated in green triangles (upregulated in T2DM) or red triangles (downregulated). **C.** Pre-miR-126 and miR-126 abundance in cell culture from hMA VSMCs was calculated as $2^{-\Delta Ct}$ using SNORD68 as housekeeping. Boxplots show Mean ± SEM data of triplicates of n = 7–11 determinations from >6 different cultures; p values were obtained with t-test. **D.** Representative microphotographs of cultured hMA VSMCs showing the expression of smooth muscle alpha actin (SMA) and SM22 protein by immunocytochemistry. Nuclei are stained with Hoechst. **E.** miR-126 abundance (normalized to SNORD68) obtained in VSMCs incubated for 24–48 h in control media (5.5 mM glucose) or high glucose-containing media (22 mM). Triplicate determinations were obtained from 3 to 4 different experiments; we observed no significant differences between 5.5 and 22 mM glucose (Kruskal–Wallis and Dunn's test).

signaling have been identified beyond membrane insulin receptors, no significant changes in IR or pIR expression were detected (Figure 3D). Altogether, these data suggest that miR-126 overexpression is an essential element in T2DM-induced epigenetic changes in VSMCs.

3.3. Effects of Kv1.3 blockade in the PM of T2DM samples and its association with miR-126

As Kv1.3 mRNA expression increased in T2DM vessels (Figure 1B), we explored Kv1.3 contribution to remodeling in these vessels. Arterial rings were incubated with 20 % FBS alone or with the Kv1.3 blocker PAP-1 (100 nmol/L). PAP-1 treatment inhibited 20 % FBS-induced remodeling in both groups, but the reduction in the I/M ratio was significantly larger in the T2DM vessels (Figure 4A). The same effect was observed in cultured VSMCs migration and proliferation (Figure 4B), where the inhibitory effects of PAP-1 remained significantly larger in T2DM cultures. Notably, the inhibitory effect of PAP-1 in the proliferation of non-T2DM VSMCs was increased by the overexpression of miR-126 (Figure 4C). These data confirm the involvement of miR-126 in the T2DM epigenetic signature of VSMCs and provide a mechanistic link to explain PAP-1 effects in T2DM.

3.4. miR-126 modulation in vascular tissues upon PM and T2DM

miR-126 dysregulation has been previously described in animal models of vascular disease in the context of T2DM [13,16]; hence, we explored its regulation upon PM in T2DM in our preparation. The miRNA qPCR array that focused on human cardiovascular disease in non-T2DM and T2DM VSMCs from fresh hMAs (Figure 5A) also identified miR-126 among the top differentially regulated miRNAs in T2DM tissue (Supplemental Table IV and supplemental Figure IV). However, in this case, miR-126 expression was smaller in contractile T2DM VSMCs (miR-126 abundance in contractile VSMCs was 17197.0 ± 5227.6 in non-T2DM and 436456 ± 1199.7 in T2DM; p = 0.015). Differences in mir-126 expression in non-T2DM and T2DM and between the contractile (fresh hMAs) and the dedifferentiated (cultured) phenotypes could reflect a different regulation of mir-126 expression upon PM, as evidenced in Figure 5B. While mir-126 is heavily downregulated in non-T2DM (17197.0 ± 5227.6 in contractile vs. 38.7 ± 7.6 in dedifferentiated, p = 0.0004), its expression does not change significantly in T2DM (4364.5 ± 1199.7 in contractile vs. 1014.9 ± 188.9 in dedifferentiated, p = 0.062), making mir-126 expression larger in the dedifferentiated phenotype of T2DM cells (36.7 ± 7.6 in non-T2DM vs. 1014.9 ± 188.9 in T2DM,

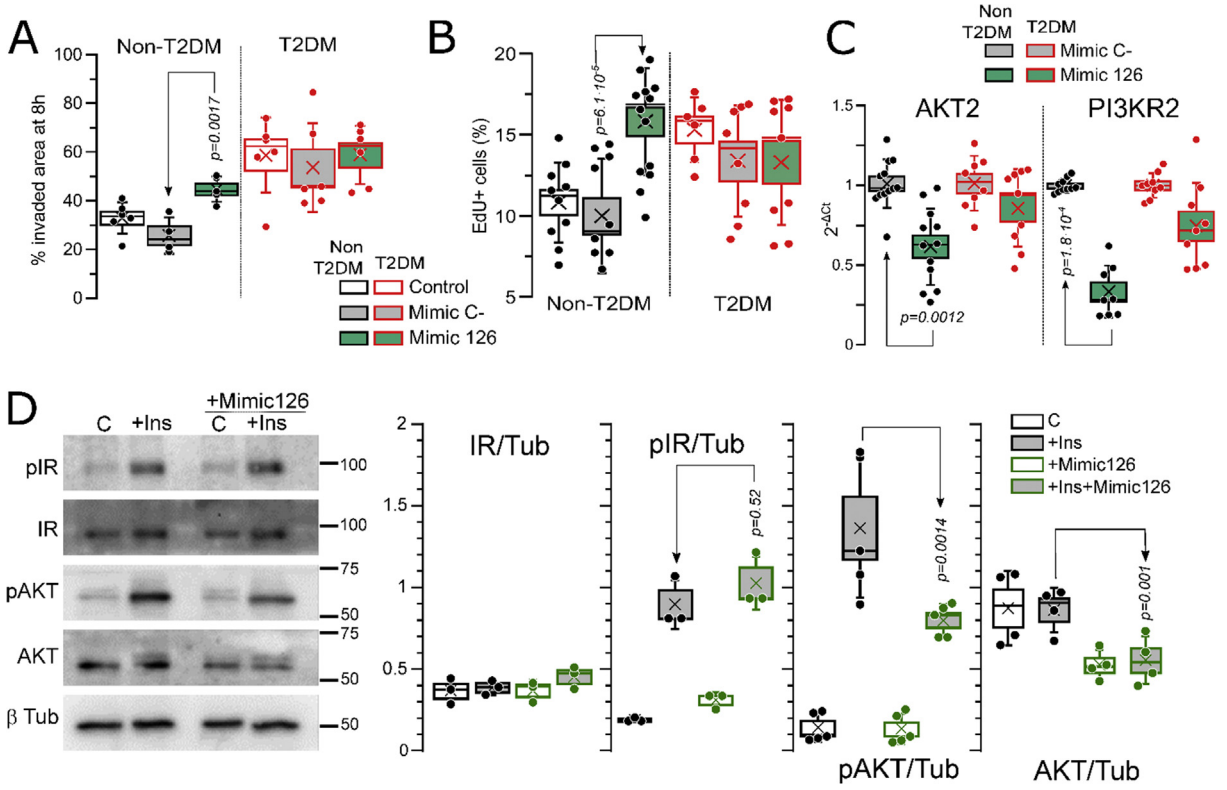

Figure 3: Effects of miR-126 gain of function in non-T2DM and T2DM VSMCs. A. Migration, expressed as % of the invaded area in a scratch assay, was studied in mock-transfected VSMCs (control) or cells transfected with mimic C- and mimic miR-126. Each box shows the mean, median, SEM, and SD of 6–8 determinations from at least 3 independent experiments, p values are from one-way ANOVA. **B.** PDGF-induced proliferation, also determined in the same conditions; n = 6–14 determinations from 3 to 6 experiments. **C.** Relative amount of PI3KR2 and AKT2 mRNA expression obtained in VSMCs in the same experimental conditions. Data are triplicates from 3 to 4 independent experiments; p values were obtained from one-way ANOVA (AKT2) or Kruskal–Wallis test (PI3KR2). **D.** Representative immunoblots of AKT, IR, and their phosphorylated forms (pAKT and pIR) from cultured non-T2DM VSMC 48 h after transfection with mimic C- or mimic miR-126. Cells were incubated for 30 min with or without insulin (100 nM) as indicated. The boxplots show normalized data (n = 4) using β-tubulin as loading control; p values were obtained from multiple comparison tests using one-way ANOVA and Tukey's test.

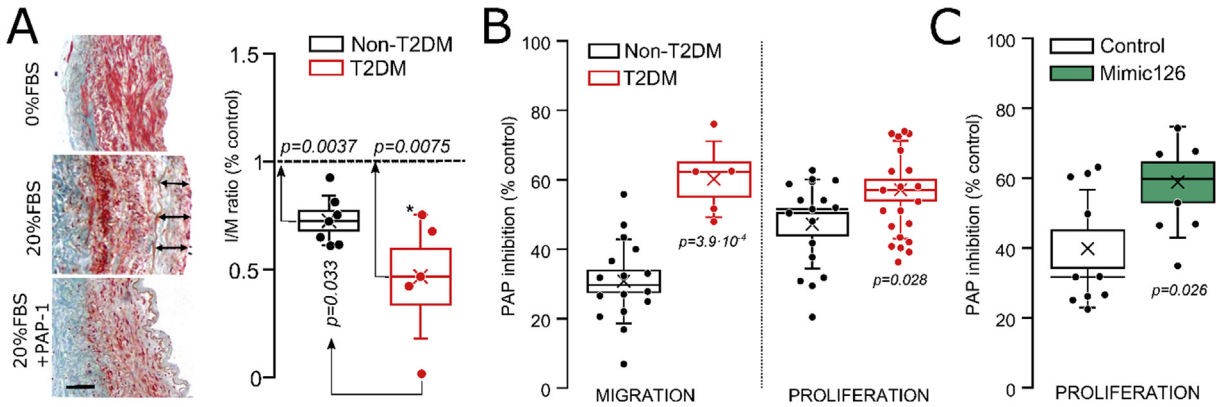

Figure 4: Effects of Kv1.3 blockade in T2DM vessel remodeling and T2DM VSMCs migration and proliferation. A. Representative microphotographs from Masson trichrome staining of T2DM hMA cultured in the indicated conditions. 10x objective. Scale bar = 100 μm. The intima/media ratio after two weeks in 20%FBS+100 nM PAP-1 was normalized to the remodeling observed in control samples (20 % FBS alone); n = 5–7 arteries, Wilcoxon–Mann–Whitney test. **B.** Effects of PAP-1 on cell migration (left panel) and cell proliferation (right panel). The inhibition of cell migration was determined 4 h after scratching a confluent monolayer of VSMCs in the presence of PAP-1. Data from n = 5–16 experiments; p values from Wilcoxon–Mann–Whitney test. The inhibition of proliferation was determined with EdU incorporation assays carried out in hMA VSMCs in the presence of PAP-1; n = 20–50 individual determinations from at least 10 independent experiments and using VSMCs from ≥4 different patients, Welch's t-test. **C.** Effect of 100 nM PAP-1 on proliferation (% of inhibition) in non-T2DM VSMCs transfected with mimic C- and mimic miR-126; n = 8–10 determinations from 5 independent experiments; p values from Wilcoxon–Mann–Whitney test.

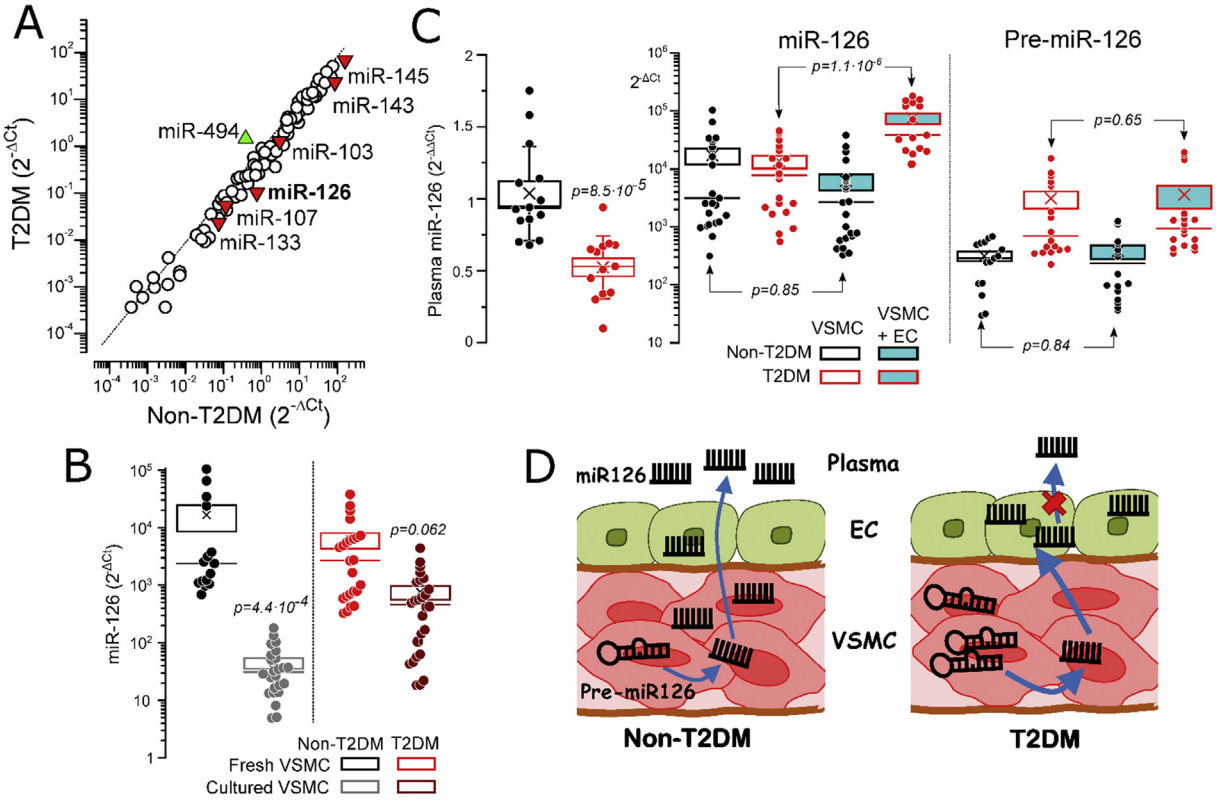

Figure 5: Regulation of miR-126 expression by PM and T2DM in human samples. A. miRNA expression levels in T2DM versus non-T2DM contractile VSMCs. Data were obtained from 2 to 3 different samples (hMA tissue without endothelium and adventitia) in each group. Selected miRNAs with expression changes >1.5 fold in T2DM are indicated with green or red triangles (up- and down-regulated, respectively). **B.** The effect of PM on the abundance of miR-126 in VSMCs from contractile (fresh VSMCs from the media layer) or proliferative (cultured VSMCs) obtained from non-T2DM (black/grey symbols) or T2DM (red/dark red symbols) was calculated as $2^{-\Delta Ct}$ using SNORD68 as housekeeping miRNA. The boxplots represent the mean, median, and SEM and show data from 7 to 12 experiments from different hMAs or VSMC cultures with triplicate determinations; p values were obtained from multiple comparisons with Kruskal–Wallis and Dunn test. **C.** The left plot represents the relative amount of miR-126 (calculated as $2^{-\Delta\Delta Ct}$) in plasma from non-T2DM and T2DM patients, using Ce-miR-39 as housekeeping and non-T2DM plasma as calibrator; n = 14 non-T2DM and n = 13 T2DM samples, p-value with Welch t-test. The other graphs show the abundance of miR-126 and its precursor pre-miR-126 in contractile VSMCs alone or with EC from non-T2DM or T2DM hMAs; n = 10–16 different samples in each group, Kruskal–Wallis and Dunn test. **D.** Scheme with the proposed explanation of the data in C.

p = 0.014). The fact that changes in miR-126 expression in contractile T2DM VSMCs resemble the changes observed on PM suggests a correlation between miR-126 expression and the differentiation state of VSMCs; so that decreases of miR-126 correspond to more dedifferentiated VSMCs.

To better understand miR-126 origin and distribution in vascular tissues, we studied its expression in plasma and vessels with or without endothelium from control and T2DM patients (Figure 5C). Smaller levels of circulating miR-126 were found in the plasma of T2DM patients as previously described [15]. miR-126 levels in the media layer (VSMCs) from non-T2DM vessels were unchanged when the endothelial layer (ECs) is present, suggesting a homogeneous distribution in the vessel wall. However, in T2DM vessels, the presence of ECs resulted in a significant increase in miR-126 expression. This could reflect either an increased miR-126 trafficking and accumulation from VSMC to EC or an increased production of miR-126 in T2DM ECs. However, pre-miR-126 expression was significantly larger in T2DM samples, independent of the presence of ECs. We propose an explanation of these data (Figure 5D), which confirm VSMCs as the main source of miR-126 in our preparation, and demonstrated that T2DM leads to an increased miR-126 synthesis. This increased miR-126 appears to be retained in the endothelium of the T2DM vessels, and this accumulation could be related to the observed decrease in miR-126 circulating levels.

3.5. Effects of Kv1.3 blockers on VSMC remodeling in a VRF mice model

To explore a clinical application of Kv1.3 blockers for preventing IH in T2DM patients, we developed a VRF mouse model to characterize the *in vivo* effects of these drugs. 6 weeks old BPH mice fed with HFD for 12 weeks exhibited significant weight gain (Figure 6A). They also developed increased fasting glucose and insulin resistance together with glucose intolerance (Figure 6B–D). Insulin tolerance test (ipITT) showed basal insulin resistance in BPH/SD mice (compared with BPN) that was exacerbated with the HFD.

We used these VRF mice to study vascular remodeling. Carotid artery ligation was used to induce lesion and remodeling. The histomorphometric analysis demonstrated that HFD induced inward remodeling of the carotid arteries, characterized by a decrease of the total area of the vessel, a concomitant increase of wall thickness, and no significant changes in wall area (Supplemental Table V). When analyzing the changes in these parameters in ligated arteries in BPH/SD, we found inward remodeling, with a reduction of the vessel area and increased vessel thickness, together with IH development that also

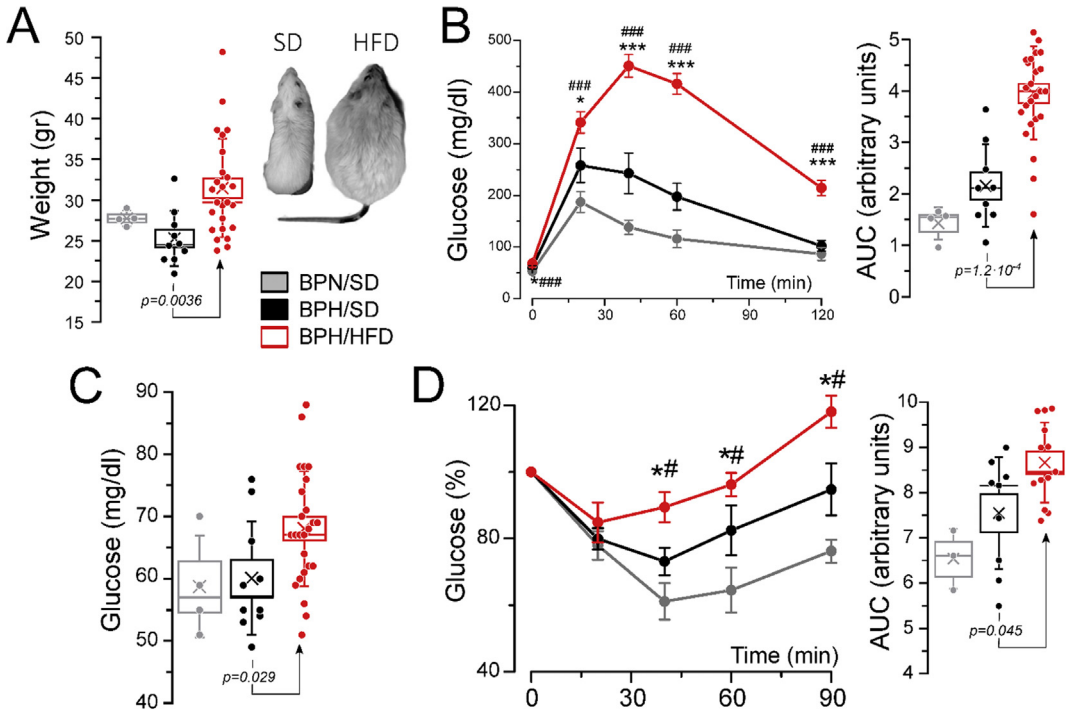

Figure 6: Generation of a VRF model. A. Average weight of BPN/SD, BPH/SD, and BPH/HFD mice. Mean, SEM, SD, and data from 9 to 25 mice per group, Kruskal—Wallis and Dunn test. A picture of an 18- week-old BPH/SD and BPH/HFD mouse is shown. **B.** ipGTT after 12 weeks of HFD. BPN/SD (n = 4), BPH/SD (n = 9), BPH/HFD (n = 25). Both the time course of blood glucose level after glucose overload in fasting animals and the area under the curve (AUC) are represented, and p values are from one-way ANOVA. **C.** Fasting blood glucose levels after 12 weeks in SD or HFD; n = 4 BPN/SD, 9 BPH/SD, and 25 BPH/HFD, one-way ANOVA. **D.** ipITT after 12 weeks of HFD. The plots show the time course of changes in blood glucose (100 % = glucose at t = 0) after insulin load, and the area under the curve (p values from one-way ANOVA); n = 4 BPN/SD, 10 BPH/SD, and 16 BPH/HFD. For B and D plots $^{*}p < 0.05$, $^{**}p < 0.01$, and $^{***}p < 0.001$ vs BPH/SD and $^{\#, \#\#, \#\#\#}$ vs BPN/SD.

determines an increase in the vessel area. In the BPH/HFD, the remodeling after carotid artery ligation did not change the total vessel area (already increased owing to the HFD), but a significant increase in the wall area compared to SD was observed. The neointima area contains dedifferentiated VSMCs, which are not labeled by SM contractile markers such as SM22 (right panels, Figure 7A). The degree of IH was best defined by the quantification of the % of stenosis and the I/M ratio, and both parameters were significantly increased in HFD lesions (Figure 7B). Of interest, as in human T2DM vessels, we found an increased expression of Kv1.3 mRNA and protein in the arteries of BPH/HFD mice (Figure 7C,D). Kv1.3 labeling increased in the muscular layer of HFD carotid arteries compared to SD vessels. A parallel increase of pERK immunoreactivity was also evident in these arteries, in agreement with the western-blot data from T2DM VSMCs (Figure 2A). Finally, the significant upregulation of pre-miR-126 in carotid and femoral arteries from HFD mice (figure 7E) indicated one more parallelism with human T2DM VSMCs (Figure 2C).

Next, we explored the effects of Kv1.3 blockers that prevented IH in BPH/HFD mice. We studied the effectiveness of this treatment compared with the application of the mTOR inhibitor EVL (1 nmol/L) — a standard treatment in clinical practice [32] — in a group of animals using mini-pumps for systemic drug delivery. Both treatments significantly decreased vessel stenosis induced by carotid ligation in BPH mice, albeit PAP-1 treatment seemed to be more potent in all treated animals (Figure 8A). The effects of PAP-1 inhibiting remodeling have been previously explored in control BPH/SD animals, with no differences between systemic or local application and no sex-related differences [19]. Here, we used the local application of PAP-1 after carotid ligation in our VRF model (BPH/HFD mice). Both the % of stenosis and the intima/media ratio were significantly decreased in the PAP-1-treated animals (Figure 8B). Moreover, the PAP-1 treatment was equally effective in SD and HFD mice (% inhibition of lumen stenosis was 41 $\pm$ 4.7 % and 37 $\pm$ 3.5 % in SD and HFD mice, respectively), but additional beneficial effects were evident in BPH/HFD mice. PAP-1 treatment reverted HFD-induced weight increase (Figure 8C); this effect appears to be specific to the HFD model, as no differences were observed in BPH/SD with PAP-1-treatment (not shown). Moreover, local application of PAP-1 fully reversed insulin resistance of BPH/HFD (Figure 8D). The ipITT area in the PAP-1 treated BPH/HFD mice was reduced to values that did not differ from those of the BPH/SD mice. Finally, while circulating, miR-126 levels were significantly reduced in BPH/HFD, as in human T2DM patients, and PAP-1 treatment could also return miR-126 levels to BPH/SD levels (Figure 8E).

4. DISCUSSION

Despite significant advances in glycemic control therapies for diabetic patients, their susceptibility to cardiovascular diseases remains a major problem. Exposure to metabolic disturbances during hyperglycemia leaves a persistent imprint on VSMCs contributing to macrovascular T2DM complications [33,34]. Importantly, the epigenetic mechanisms contributing to metabolic memory of VSMC are potentially reversible [35]; therefore, their identification and removal offer promising therapeutical opportunities.

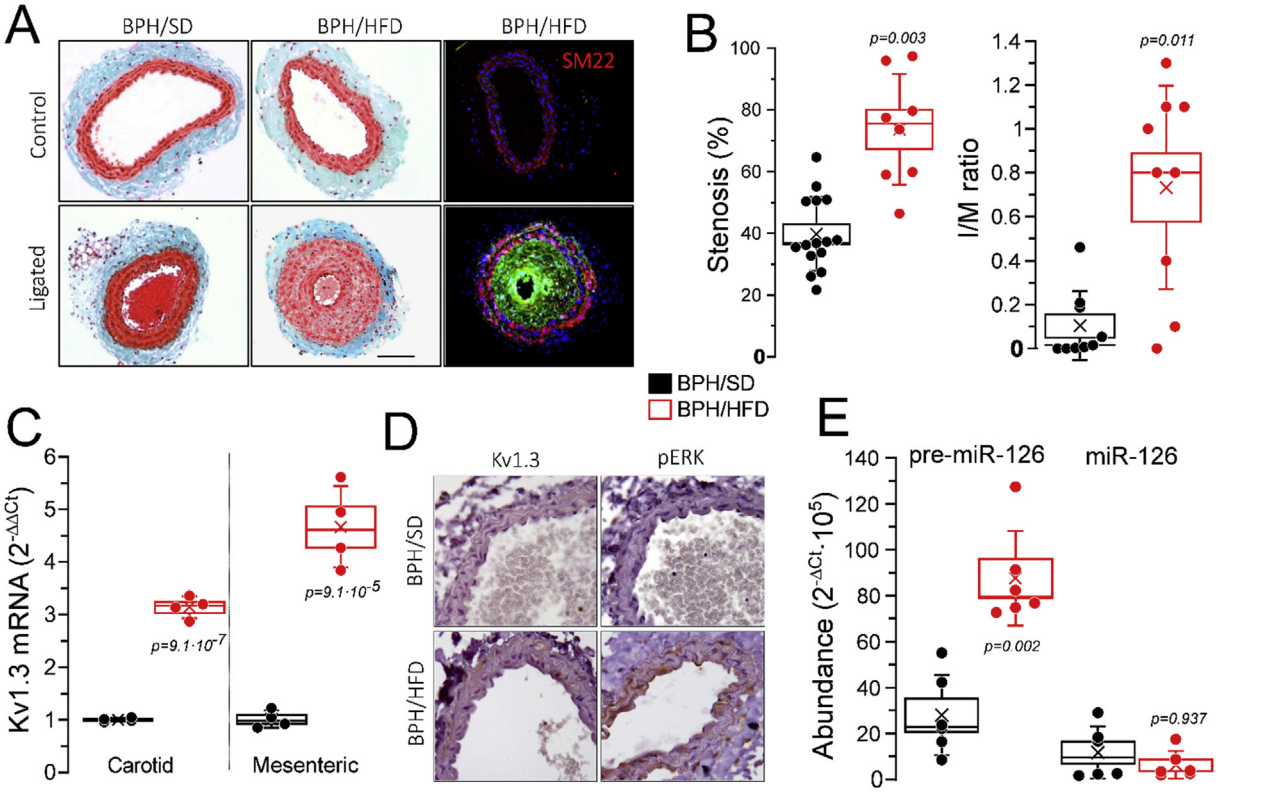

Figure 7: Characterization of vascular remodeling in the VRF mice model A. Representative images of control and ligated carotid arteries from BPH/SD and BPH/HFD mice. The right and middle panels show Masson trichrome staining of paraffin-embedded sections. 20x objective. Scale bar 100 μm. The left panel shows SM22 labeling (red) in control and ligated arteries, with elastic lamina autofluorescence in green, from the same arteries of the middle panel, illustrating the limit between media (SM22 positive) and intima layer (SM22 negative). **B.** Boxplots representing % of stenosis (left) and intima to media ratio (right) of BPH/SD (black) and BPH/HFD (red) ligated carotid arteries. Analysis was performed in 3 different cross-sections of 9 mice in each group; p values from Welch's two sample t-test (% stenosis) and Wilcoxon—Mann—Whitney test (I/M ratio). **C.** Kv1.3 mRNA relative expression, using RPL18 as housekeeping and BPH/SD as calibrator. n = 4; p values from t-test. **D.** Kv1.3 and pERK immunolabeling in sections of control carotid arteries from BPH/SD and BPH/HFD mice. 40x objective. **E.** Pre-miR-126 and miR-126 abundance ($2^{-\Delta Ct}$) in carotid and mesenteric arteries, using SNORD68 as endogenous control; n = 3 independent samples per group; p values from Wilcoxon—Mann—Whitney test.

Our study explored some of the mechanisms involved in the T2DM increased vascular risk, providing some clinically relevant conclusions. First, we explored the effect of T2DM in the remodeling of human vessels using organ culture of hMA samples, to determine that these vessels exhibited larger IH lesions, increased Kv1.3 mRNA expression, and elevated sensitivity to the Kv1.3 blocker PAP-1, compared to non-T2DM vessels. Second, we confirmed that T2DM-induced epigenetic changes in human vessels remain *ex vivo*, showing increased proliferation and migration rates, changes in specific growth factors' activated pathways, and an altered miRNA signature. We demonstrated that miR-126 upregulation mimics many of the features of the T2DM phenotype in non-T2DM cultured VSMCs, including the increased contribution of Kv1.3 channels to proliferation. Third, we developed a mouse model of VRF (including T2DM) using BPH mice fed with HFD, in which we observed changes in vessel remodeling after vascular injury, increased VSMCs expression of Kv1.3, pre-miR-126, and decreased plasmatic levels of miR-126 comparable to those observed in T2DM patients. Interestingly, PAP-1 treatment after vascular lesion in T2DM mice not only prevented IH in the injured vessel, but also showed additional beneficial metabolic effects. In summary, we disclose some of the mechanisms involved in metabolic memory of human T2DM VSMCs, which contribute to the enhanced effects of Kv1.3 blockers in the prevention of IH after vascular surgery in T2DM vessels.

4.1. Human T2DM VSMC show epigenetic changes

T2DM metabolic memory is a poorly understood phenomenon with major challenges in treating diabetes. T2DM-induced epigenetic changes in VSMC from different T2DM animal models include DNA methylation, post-translational histone modifications, and miRNA dysregulation [13,16,24,30,35—37]. Except for the study of Coleman [38], which uses human T2DM VSMCs, the data from animal models has been validated in healthy human VSMCs treated with high glucose, as an *in vitro* model of hyperglycemia [14,30]. Here, we studied T2DM-induced epigenetic changes in primary VSMCs obtained from non-T2DM and T2DM patients and correlated them with the IH development of vessel rings in organ culture. Even considering all the potential limitations of cultured VSMCs, they offer a nontrivial improvement over the previous models, as we found that T2DM-induced changes in miRNA expression could not be reproduced in healthy VSMCs that were cultured in high glucose media (Figure 2E).

4.2. miRNAs profile in T2DM vessels

Our miRNA PCR array provided several miRNAs differentially regulated in cultured T2DM VSMCs. Some of them had been previously described, although there is huge variability in the literature: 1) There are several studies directed to identify risk stratification or prognosis biomarkers which only explore circulating miRNAs (but not their expression in vascular cells [15,25,39]). Plasma miRNAs may not

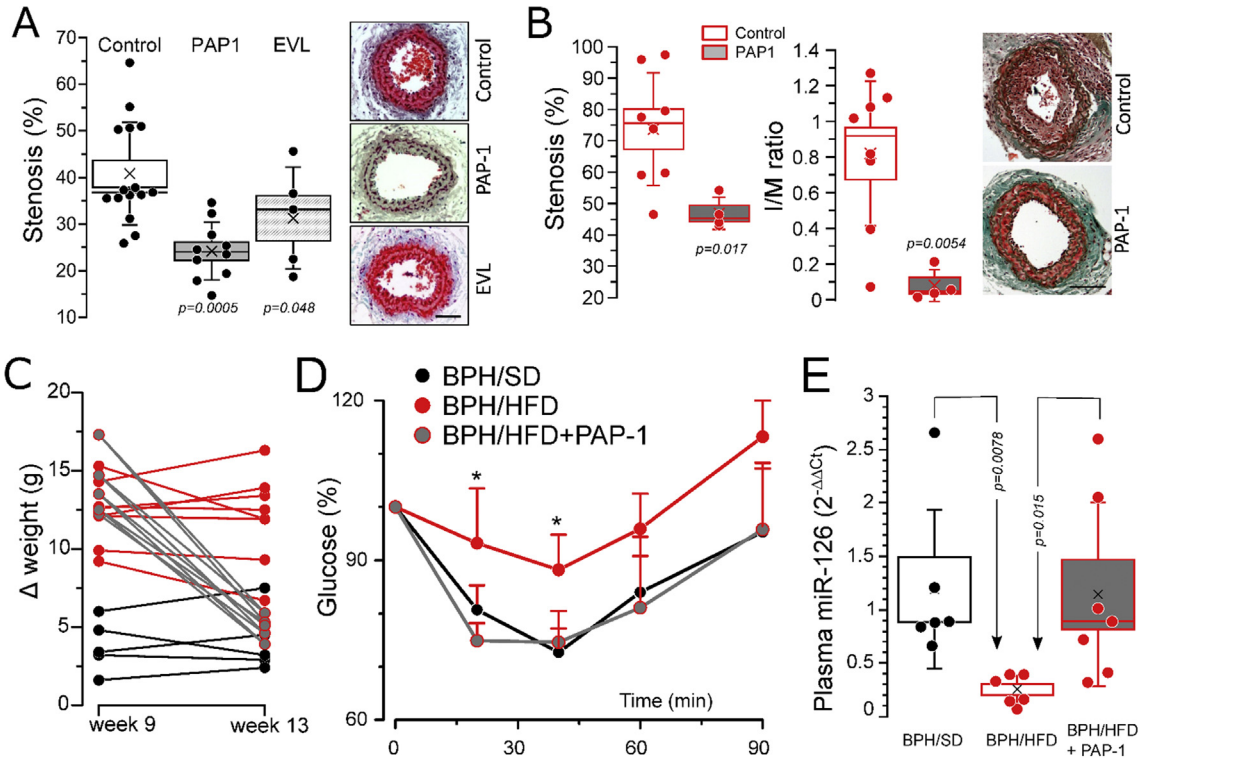

Figure 8: Effects of Kv1.3 blockers *in vivo*. A. Effect of systemic application of PAP-1 and EVL on vascular remodeling. The plot shows the % stenosis of the ligated arteries in the indicated conditions (control = mini-pump with vehicle). Representative microphotographs are shown. 20x objective (scale bar = 100 μm). Data from n = 5–15 BPH/SD mice per group; p values from one-way ANOVA. **B.** Microphotographs of untreated BPH/HFD ligated carotid arteries (control, left) or treated with PAP-1 in-situ (Right). 20x magnification. Scale bar = 100 μm. The percentage stenosis (left) and intima/media ratio (right) from n = 8 control and n = 4 PAP-1-treated mice is shown in the boxplots; p values from t-test. **C.** Weight gain of each mice from week 9 (before carotid ligation) to week 13 (after 4-weeks treatment with vehicle or PAP-1). **D**. ipITT showing the time course of changes in blood glucose after insulin load; n = 5–6 mice per group. *p < 0.05 vs BPH/SD. **E.** Relative amount of plasma miR-126 levels, calculated using Ce-miR-39 as housekeeping and BPH/SD values as calibrator; p values from Kruskal–Wallis and Dunn test. N = 6–7 mice per group.

necessarily reflect local tissue levels. Nevertheless, all these studies point to the decrease of circulating miR-126 as a consistent biomarker of cardiovascular risk in T2DM, a finding confirmed here in plasma from both T2DM patients and VRF mice. 2) Other studies used high-throughput miRNA in VSMCs from T2DM animal models, and either vessel or cultured VSMCs, (but not both) to explore the impact of PM in T2DM [13,16]. Again, despite the enormous differences among studies, they link miR-126 with vascular pathologies and T2DM. Our data underwrite these findings, expanding them to the regulation of miR-126 in VSMCs from T2DM patients.

4.3. miR-126 role in T2DM vessels

miR-126 plays a central role in endothelial cells (ECs) homeostasis, inducing angiogenesis during embryogenesis and tissue repair [40]. In VSMCs, miR-126 has been postulated as a paracrine mediator secreted by ECs which modulates gene expression and function towards atherogenic phenotype [41,42]. However, while some studies showed that systemic depletion of miR-126 in mice inhibits neointimal lesion induced by carotid ligation [43], others stated that endothelial miR-126 reduces IH and vascular remodeling [44,45]. An essential role of the miR-126-5p strand (and not miR-126-3p, which is the one studied here) in the regulation of EC proliferation has been demonstrated [41]. Based on these, a differential role in EC functions of the two miR-126 strands could account for the observed discrepancies.

In contrast to the lower levels of plasmatic miR-126 associated with T2DM patients [15] and animal models [28], we found that VSMCs express miR-126 and that T2DM increased its expression. The higher miR-126 expression found in T2DM VSMCs does not imply higher circulating levels, as miR-126 could remain in VSMCs (as it appears to be the case in our VSMC cultures) or be secreted from VSMCs to EC (as we hypothesize in the case of contractile VSMC in the vessel wall, refer Figure 5D). The miR-126 gain of function studies provided very clear-cut results: miR-126 overexpression augmented proliferation and migration rates only in non-T2DM cells (Figure 3A,B). T2DM VSMCs showed higher rates of migration and proliferation (Figure 1C,D), so we postulate that miR-126 overexpression can confer the "diabetic" phenotype to non-T2DM cells. Moreover, in non-T2DM VSMCs, miR-126 mimic led to a decrease in the expression of two known miR-126 targets, AKT-2 (mRNA and protein) and PI3KR2 (mRNA). These results fit nicely with the downregulation of the PI3K/AKT pathway on T2DM [23,24] (refer also Figure 2A), confirming that miR-126 upregulation contributes to the T2DM epigenetic signature of cultured VSMCs.

Many other targets of miR-126 were unchanged in our cells (Supplemental Table III), most likely because of tissue-specific miRNA targets and miRNA effects. This could explain the differences in miR-126 effects between our preparation (where miR-126 is acting on VSMCs) and previous works exploring ECs miR-126. EC-derived miR-126 has been proposed to increase atherogenesis [43], VSMCs turnover during angiogenesis [42], or decreased proliferation and migration in VSMCs. These effects of miR-126 were mediated by target genes that were not affected in our preparation, including FOXO3, IRS-1, SPRED1, or EGFL7 among others.

4.4. Kv1.3 role in T2DM vessels

Our data suggest that changes in the relative contribution of PI3K/AKT/mTOR and MEK/ERK axis in T2DM VSMCs represent the link between miR-126 upregulation and the enhanced functional expression of Kv1.3 channels. Both changes contribute to the increased activation of the MEK/ERK signaling pathway in T2DM VSMCs (refer graphical abstract). This hypothesis was confirmed by the increased contribution of Kv1.3 channels on the proliferation on miR-126 overexpression in non-T2DM VSMCs (Figure 4C).

To expand these findings to other clinically relevant preparation, we created a VRF model (BPH/HFD) including insulin resistance and T2DM. As in human T2DM vessels, BPH/HFD vessels showed increased expression of Kv1.3 mRNA, suggesting a change toward a more dedifferentiated phenotype [46]. HFD induced vessel remodeling, exacerbating IH after carotid ligation, similar to other genetic or diet-induced models of T2DM [24,47,48], and PAP-1 treatment was also effective in preventing IH and vascular remodeling in BPH/HFD injured vessels. Additional beneficial effects of local PAP-1 treatment in BPH/HFD mice included decreased weight gain and removal of insulin resistance, together with the normalization of circulating miR-126 levels in these animals. The contribution of Kv1.3 to the pathways that regulate energy homeostasis and body weight has been reported, as Kv1.3KO mice showed increased basal metabolic rate and enhanced insulin sensitivity, being resistant to diet-induced obesity [49,50]. Consistently, Kv1.3 blockers have been described to counteract the negative effects of increased caloric intake in mice fed with HFD, reducing weight gain and associated inflammation and improving glucose tolerance [51]. Thus, we found that the obesity-inducing diet enhanced sensitivity to Kv1.3 inhibition as Kv1.3 blockade did not alter weight gain in BPH/SD mice.

4.5. Conclusions

The present study uncovers one mechanism that contributes to exacerbated restenosis in T2DM patients. We found increased Kv1.3 expression in T2DM vessels. Our data also indicate that miR-126 upregulation is an essential element that contributes to the metabolic memory of T2DM VSMCs. Although Kv1.3 channels are not targets of miR-126, the upregulation of miR-126 potentiates Kv1.3-dependent mechanisms in T2DM vessels, so that Kv1.3 inhibition is more efficient in preventing remodeling in T2DM patients.

4.6. Study limitations

Our data exclude the Kv1.3 channel as a target of miR-126; hence, further research will be required to explore the mechanisms involved in Kv1.3 upregulation observed in both human and mice diabetic VSMC. Also, more research is granted to fully understand the molecular interactions and the crosstalk between miR-126 modulated pathways and Kv1.3 signaling pathways in T2DM VSMCs, and their contribution to remodel diseased vessels.

AUTHOR CONTRIBUTIONS

Conceptualization: MAM, PC, SA, IC, JRLL, and MTPG; Methodology and investigation MAM, PC, SME, MF, IC; Formal analysis and validation. MAM, PC, SA, IC, JRLL, and MTPG; Visualization; MAM, PC, JRLL and MTPG; Supervision: PC, SA, IC, JRLL, and MTPG; Funding acquisition: SA, IC, JRLL, and MTPG; Writing-original draft: MAM, PC, JRLL and MTPG; Writing-review & editing: MAM, PC, SME, MF, SA, IC, JRLL, and MTPG.

AVAILABILITY OF DATA AND MATERIALS

The data that support the findings of this study are available from the corresponding author upon reasonable request.

ACKNOWLEDGMENTS

We thank Esperanza Alonso for excellent technical assistance, and Drs. Alberto San Román, Juan Bustamante, and all the personnel of the Cardiac Surgery Unit of the HCU de Valladolid for providing the vessel and blood samples.

Supported by the Spanish Ministerio de Economía y Competitividad (MINECO) [BFU2016-75360-R to MTP-G and JRL-L, SAF2016-77871-C2-1-R to IC-C] and Junta de Castilla y León [VA114P17, VA172P20 to MTP-G] and Programa Estratégico IBGM), Escalera de Excelencia, Junta de Castilla y León (CLU-2019-02). SA was supported by Novo Nordisk Foundation (grant 34366), Swedish Research Council (grants 2017—00860, 2020-01145), Swedish Heart and Lung Foundation grant (20200322), and the Crafoord and Magnus Bergvall Foundations. MAM is a predoctoral fellow of the UVa-Santander, SME holds a predoctoral fellowship of the JCyL.

CONFLICT OF INTEREST

Authors declare that they have no competing interests.

APPENDIX A.SUPPLEMENTARY DATA

Supplementary data to this article can be found online at https://doi.org/10.1016/j.molmet.2021.101306.

REFERENCES

[1] Aronson, D., Edelman, E.R., 2010. Revascularization for coronary artery disease in diabetes mellitus: angioplasty, stents and coronary artery bypass grafting. Reviews in Endocrine & Metabolic Disorders 11(1):75—86. https://doi.org/10.1007/s11154-010-9135-3.

[2] Brown, A., Reynolds, L.R., Bruemmer, D., 2010. Intensive glycemic control and cardiovascular disease: an update. Nature Reviews Cardiology, 369—375. https://doi.org/10.1038/nrcardio.2010.35.

[3] Skyler, J.S., Bergenstal, R., Bonow, R.O., Buse, J., Deedwania, P., Gale, E.A.M., et al., 2009. Intensive glycemic control and the prevention of cardiovascular events: implications of the accord, advance, and VA diabetes trials. A position statement of the American diabetes association and a scientific statement of the American college of cardiology foundation and the American heart association. Journal of the American College of Cardiology, 298—304. https://doi.org/10.1016/j.jacc.2008.10.008.

[4] Cooper, M.E., El-Osta, A., Allen, T.J., Watson, A.M.D., Thomas, M.C., Jandeleit-Dahm, K.A.M., 2018. Metabolic karma-the atherogenic legacy of diabetes: the 2017 edwin bierman award lecture. Diabetes 67(5):785—790. https://doi.org/10.2337/dbi18-0010.

[5] Intine, R.V., Sarras, M.P., 2012. Metabolic memory and chronic diabetes complications: potential role for epigenetic mechanisms. Current Diabetes Reports 12(5):551—559. https://doi.org/10.1007/s11892-012-0302-7.

[6] Alexander, M.R., Owens, G.K., 2012. Epigenetic control of smooth muscle cell differentiation and phenotypic switching in vascular development and disease. Annual Review of Physiology 74(1):13—40. https://doi.org/10.1146/annurev-physiol-012110-142315.

[7] Owens, G.K., Kumar, M.S., Wamhoff, B.R., 2004. Molecular regulation of vascular smooth muscle cell differentiation in development and disease.

Physiological Reviews 84:767–801. https://doi.org/10.1152/physrev.00041.2003.

[8] Cidad, P., Moreno-Domínguez, A., Novensá, L., Roqué, M., Barquín, L., Heras, M., et al., 2010. Characterization of ion channels involved in the proliferative response of femoral artery smooth muscle cells. Arteriosclerosis, Thrombosis, and Vascular Biology 30(6):1203–1211. https://doi.org/10.1161/ATVBAHA.110.205187.

[9] Cidad, P., Miguel-Velado, E., Ruiz-McDavitt, C., Alonso, E., Jiménez-Pérez, L., Asuaje, A., et al., 2015. Kv1.3 channels modulate human vascular smooth muscle cells proliferation independently of mTOR signaling pathway. Pfluegers Archiv European Journal of Physiology 467(8):1711–1722. https://doi.org/10.1007/s00424-014-1607-y.

[10] Cheong, A., Li, J., Sukumar, P., Kumar, B., Zeng, F., Riches, K., et al., 2011. Potent suppression of vascular smooth muscle cell migration and human neointimal hyperplasia by KV1.3 channel blockers. Cardiovascular Research 89(2):282–289. https://doi.org/10.1093/cvr/cvq305.

[11] Cidad, P., Novensà, L., Garabito, M., Batlle, M., Dantas, A.P.P., Heras, M., et al., 2014. K+ channels expression in hypertension after arterial injury, and effect of selective Kv1.3 blockade with PAP-1 on intimal hyperplasia formation. Cardiovascular Drugs and Therapy 28(6):501–511. https://doi.org/10.1007/s10557-014-6554-5.

[12] Arévalo-Martínez, M., Cidad, P., García-Mateo, N., Moreno-Estar, S., Serna, J., Fernández, M., et al., 2019. Myocardin-dependent Kv1.5 channel expression prevents phenotypic modulation of human vessels in organ culture. Arteriosclerosis, Thrombosis, and Vascular Biology 39(12):E273–E286. https://doi.org/10.1161/ATVBAHA.119.313492.

[13] Torella, D., Iaconetti, C., Tarallo, R., Marino, F., Giurato, G., Veneziano, C., et al., 2018. miRNA regulation of the hyperproliferative phenotype of vascular smooth muscle cells in diabetes. Diabetes 67(12):2554–2568. https://doi.org/10.2337/DB17-1434.

[14] Togliatto, G., Dentelli, P., Rosso, A., Lombardo, G., Gili, M., Gallo, S., et al., 2018. PDGF-BB carried by endothelial Cell-derived extracellular vesicles reduces vascular smooth muscle cell apoptosis in diabetes. Diabetes 67(4):704–716. https://doi.org/10.2337/db17-0371.

[15] Zampetaki, A., Kiechl, S., Drozdov, I., Willeit, P., Mayr, U., Prokopi, M., et al., 2010. Plasma microRNA profiling reveals loss of endothelial miR-126 and other microRNAs in type 2 diabetes. Circulation Research 107(6):810–817. https://doi.org/10.1161/CIRCRESAHA.110.226357.

[16] Reddy, M.A., Das, S., Zhuo, C., Jin, W., Wang, M., Lanting, L., et al., 2016. Regulation of vascular smooth muscle cell dysfunction under diabetic conditions by MIR-504. Arteriosclerosis, Thrombosis, and Vascular Biology 36(5):864–873. https://doi.org/10.1161/ATVBAHA.115.306770.

[17] Miguel-Velado, E., Moreno-Domínguez, A., Colinas, O., Cidad, P., Heras, M., Pérez-García, M.T.T., et al., 2005. Contribution of Kv channels to phenotypic remodeling of human uterine artery smooth muscle cells. Circulation Research 97(12):1280–1287. https://doi.org/10.1161/01.RES.0000194322.91255.13.

[18] Villa-Pérez, P., Merino, B., Fernández-Díaz, C.M., Cidad, P., Lobatón, C.D., Moreno, A., et al., 2018. Liver-specific ablation of insulin-degrading enzyme causes hepatic insulin resistance and glucose intolerance, without affecting insulin clearance in mice. Metabolism Clinical and Experimental 88:1–11. https://doi.org/10.1016/j.metabol.2018.08.001.

[19] Moreno-Estar, S., Serrano, S., Arévalo-Martínez, M., Cidad, P., López-López, J.R., Santos, M., et al., 2020. Elastin-like recombinamer-based devices releasing Kv1.3 blockers for the prevention of intimal hyperplasia: an in vitro and in vivo study. Acta Biomaterialia 115:264–274. https://doi.org/10.1016/j.actbio.2020.07.053.

[20] Roque, M., Fallon, J.T., Badimon, J.J., Zhang, W.X., Taubman, M.B., Reis, E.D., 2000. Mouse model of femoral artery denudation injury associated with the rapid accumulation of adhesion molecules on the luminal surface and recruitment of neutrophils. Arteriosclerosis, Thrombosis, and Vascular Biology 20(2):335–342. https://doi.org/10.1161/01.ATV.20.2.335.

[21] Livak, K.J., Schmittgen, T.D., 2001. Analysis of relative gene expression data using real-time quantitative PCR and the 2(-ΔΔCT) method. Methods 25(4):402–408. https://doi.org/10.1006/meth.2001.1262.

[22] Sandu, O.A., Ragolia, L., Begum, N., 2000. Diabetes in the Goto-Kakizaki rat is accompanied by impaired insulin-mediated myosin-bound phosphatase activation and vascular smooth muscle cell relaxation. Diabetes 49(12):2178–2189. https://doi.org/10.2337/diabetes.49.12.2178.

[23] Kim, J.A., Montagnani, M., Kwang, K.K., Quon, M.J., 2006. Reciprocal relationships between insulin resistance and endothelial dysfunction: molecular and pathophysiological mechanisms. Circulation 113(15):1888–1904. https://doi.org/10.1161/CIRCULATIONAHA.105.563213.

[24] Lightell, D.J., Moss, S.C., Woods, T.C., 2018. Upregulation of miR-221 and -222 in response to increased extracellular signal-regulated kinases 1/2 activity exacerbates neointimal hyperplasia in diabetes mellitus. Atherosclerosis 269:71–78. https://doi.org/10.1016/j.atherosclerosis.2017.12.016.

[25] Olivieri, F., Spazzafumo, L., Bonafè, M., Recchioni, R., Prattichizzo, F., Marcheselli, F., et al., 2015. MiR-21-5p and miR-126a-3p levels in plasma and circulating angiogenic cells: relationship with type 2 diabetes complications. Oncotarget 6(34):35372–35382. https://doi.org/10.18632/oncotarget.6164.

[26] Jansen, F., Wang, H., Przybilla, D., Franklin, B.S., Dolf, A., Pfeifer, P., et al., 2016. Vascular endothelial microparticles-incorporated microRNAs are altered in patients with diabetes mellitus. Cardiovascular Diabetology 15(1):49. https://doi.org/10.1186/s12933-016-0367-8.

[27] Wu, K., Yang, Y., Zhong, Y., Ammar, H.M., Zhang, P., Guo, R., et al., 2016. The effects of microvesicles on endothelial progenitor cells are compromised in type 2 diabetic patients via downregulation of the miR-126/VEGFR2 pathway. American Journal of Physiology - Endocrinology And Metabolism 310(10):E828–E837. https://doi.org/10.1152/ajpendo.00056.2016.

[28] Venkat, P., Cui, C., Chopp, M., Zacharek, A., Wang, F., Landschoot-Ward, J., et al., 2019. MiR-126 mediates brain endothelial cell exosome treatment–induced neurorestorative effects after stroke in type 2 diabetes mellitus mice. Stroke 50(10):2865–2874. https://doi.org/10.1161/STROKEAHA.119.025371.

[29] Santulli, G., 2015. microRNAs distinctively regulate vascular smooth muscle and endothelial cells: functional implications in angiogenesis, atherosclerosis, and in-stent restenosis. In: Advances in experimental medicine and biology, vol. 887. Springer New York LLC. p. 53–77.

[30] Villeneuve, L.M., Reddy, M.A., Lanting, L.L., Wang, M., Meng, L., Natarajan, R., 2008. Epigenetic histone H3 lysine 9 methylation in metabolic memory and inflammatory phenotype of vascular smooth muscle cells in diabetes. Proceedings of the National Academy of Sciences of the United States of America 105(26):9047–9052. https://doi.org/10.1073/pnas.0803623105.

[31] Jansen, F., Yang, X., Hoelscher, M., Cattelan, A., Schmitz, T., Proebsting, S., et al., 2013. Endothelial microparticle-mediated transfer of MicroRNA-126 promotes vascular endothelial cell repair via SPRED1 and is abrogated in glucose-damaged endothelial microparticles. Circulation 128(18):2026–2038. https://doi.org/10.1161/CIRCULATIONAHA.113.001720.

[32] Picard, F., Pighi, M., de Hemptinne, Q., Airaksinen, J., Vinco, G., de Pommereau, A., et al., 2019. Comparison of the biodegradable polymer everolimus-eluting stent with contemporary drug-eluting stents: a systematic review and meta-analysis. International Journal of Cardiology 278:51–56. https://doi.org/10.1016/j.ijcard.2018.11.113.

[33] El-Osta, A., Brasacchio, D., Yao, D., Pocai, A., Jones, P.L., Roeder, R.G., et al., 2008. Transient high glucose causes persistent epigenetic changes and altered gene expression during subsequent normoglycemia. Journal of Experimental Medicine 205(10):2409–2417. https://doi.org/10.1084/jem.20081188.

[34] Porter, K.E., Riches, K., 2015. Vascular smooth muscle as a target for novel therapeutics. Current Diabetes Reports 15(10):1—11. https://doi.org/10.1007/s11892-015-0647-9.

[35] Stratton, M.S., Farina, F.M., Elia, L., 2019. Epigenetics and vascular diseases. Journal of Molecular and Cellular Cardiology 133:148—163. https://doi.org/10.1016/j.yjmcc.2019.06.010.

[36] Zhong, Q., Kowluru, R.A., 2011. Epigenetic changes in mitochondrial superoxide dismutase in the retina and the development of diabetic retinopathy. Diabetes 60(4):1304—1313. https://doi.org/10.2337/db10-0133.

[37] Wegner, M., Neddermann, D., Piorunska-Stolzmann, M., Jagodzinski, P.P., 2014. Role of epigenetic mechanisms in the development of chronic complications of diabetes. Diabetes Research and Clinical Practice 105(2):164—175. https://doi.org/10.1016/j.diabres.2014.03.019.

[38] Coleman, C.B., Lightell, D.J., Moss, S.C., Bates, M., Parrino, P.E., Woods, T. C., 2013. Elevation of miR-221 and -222 in the internal mammary arteries of diabetic subjects and normalization with metformin. Molecular and Cellular Endocrinology 374(1—2):125—129. https://doi.org/10.1016/j.mce.2013.04.019.

[39] Banerjee, J., Nema, V., Dhas, Y., Mishra, N., 2017. Role of MicroRNAs in type 2 diabetes and associated vascular complications. Biochimie 139:9—19. https://doi.org/10.1016/j.biochi.2017.05.007.

[40] Chistiakov, D.A., Orekhov, A.N., Bobryshev, Y.V., 2016. The role of miR-126 in embryonic angiogenesis, adult vascular homeostasis, and vascular repair and its alterations in atherosclerotic disease. Journal of Molecular and Cellular Cardiology 97:47—55. https://doi.org/10.1016/j.yjmcc.2016.05.007.

[41] Schober, A., Nazari-Jahantigh, M., Wei, Y., Bidzhekov, K., Gremse, F., Grommes, J., et al., 2014. MicroRNA-126-5p promotes endothelial proliferation and limits atherosclerosis by suppressing Dlk1. Nature Medicine 20(4):368—376. https://doi.org/10.1038/nm.3487.

[42] Kuhnert, F., Mancuso, M.R., Hampton, J., Stankunas, K., Asano, T., Chen, C.Z., et al., 2008. Attribution of vascular phenotypes of the murine Egf17 locus to the microRNA miR-126. Development 135(24):3989—3993. https://doi.org/10.1242/dev.029736.

[43] Zhou, J., Li, Y.-S., Nguyen, P., Wang, K.-C., Weiss, A., Kuo, Y.-C., et al., 2013. Regulation of vascular smooth muscle cell turnover by endothelial cell—secreted MicroRNA-126. Circulation Research 113(1):40—51. https://doi.org/10.1161/CIRCRESAHA.113.280883.

[44] Jansen, F., Zietzer, A., Stumpf, T., Flender, A., Schmitz, T., Nickenig, G., et al., 2017. Endothelial microparticle-promoted inhibition of vascular remodeling is abrogated under hyperglycaemic conditions. Journal of Molecular and Cellular Cardiology 112:91—94. https://doi.org/10.1016/J.YJMCC.2017.09.004.

[45] Izuhara, M., Kuwabara, Y., Saito, N., Yamamoto, E., Hakuno, D., Nakashima, Y., et al., 2017. Prevention of neointimal formation using miRNA-126-containing nanoparticle-conjugated stents in a rabbit model. PloS One 12(3). https://doi.org/10.1371/journal.pone.0172798.

[46] López-López, J.R., Cidad, P., Pérez-García, M.T., 2018. Kv channels and vascular smooth muscle cell proliferation. Microcirculation 25(1). https://doi.org/10.1111/micc.12427.

[47] Xi, T., Jin, F., Zhu, Y., Wang, J., Tang, L., Wang, Y., et al., 2017. MicroRNA-126-3p attenuates blood-brain barrier disruption, cerebral edema and neuronal injury following intracerebral hemorrhage by regulating PIK3R2 and Akt. Biochemical and Biophysical Research Communications 494(1—2):144—151. https://doi.org/10.1016/J.BBRC.2017.10.064.

[48] Hubert, A., Bochenek, M.L., Schütz, E., Gogiraju, R., Münzel, T., Schäfer, K., 2017. Selective deletion of leptin signaling in endothelial cells enhances neointima formation and phenocopies the vascular effects of diet-induced obesity in mice. Arteriosclerosis, Thrombosis, and Vascular Biology 37(9):1683—1697. https://doi.org/10.1161/ATVBAHA.117.309798.

[49] Xu, J., Wang, P., Li, Y., Li, G., Kaczmarek, L.K., Wu, Y., et al., 2004. The voltage-gated potassium channel Kv1.3 regulates peripheral insulin sensitivity. Proceedings of the National Academy of Sciences of the United States of America 101(9):3112—3117. https://doi.org/10.1073/pnas.0308450100.

[50] Choi, B.H., Hahn, S.J., 2010. Kv1.3: a potential pharmacological target for diabetes. Acta Pharmacologica Sinica 31(9):1031—1035. https://doi.org/10.1038/aps.2010.133.

[51] Upadhyay, S.K., Eckel-Mahan, K.L., Mirbolooki, M.R., Tjong, I., Griffey, S.M., Schmunk, G., et al., 2013. Selective Kv1.3 channel blocker as therapeutic for obesity and insulin resistance. Proceedings of the National Academy of Sciences 110(24):E2239—E2248. https://doi.org/10.1073/pnas.1221206110.

